

Linking in domain-swapped protein dimers

Marco Baiesi^{1,2,*}, Enzo Orlandini^{1,2}, Antonio Trovato^{1,3}, Flavio Seno^{1,3},

1 Department of Physics and Astronomy, University of Padova, Padova, Italy

2 INFN - Sezione di Padova, Padova, Italy

3 CNISM, Padova, Italy

* E-mail: Corresponding baiesi@pd.infn.it

Abstract

The presence of physical knots has been observed in a small fraction of single-domain proteins and related to their thermodynamic and kinetic properties. The entanglement between different chains in multimeric protein complexes, as captured by their linking number, may as well represent a significant topological feature. The exchanging of identical structural elements typical of domain-swapped proteins make them suitable candidates to validate this possibility.

Here we analyze 110 non redundant domain-swapped dimers filtered from the *3Dswap* and *Proswap* databases, by keeping only structures not affected by the presence of holes along the main backbone chain. The linking number G' determined by Gauss integrals on the C_α backbones is shown to be a solid and efficient tool for quantifying the mutual entanglement, also due to its strong correlation with the topological linking averaged over many closures of the chains.

Our analysis evidences a quite high fraction of chains with a significant linking, that is with $|G'| > 1$. We report that Nature promotes configurations with $G' < 0$ and surprisingly, it seems to suppress linking of long proteins. While proteins composed of about 100 residues can be well linked in the swapped dimer form, this is not observed for much longer chains. Upon dissociation of a few dimers via numerical simulations, we observe an exponential decay of the linking number with time, providing an additional useful characterization of the entanglement within swapped dimers. Our results provide a novel and robust topology-based classification of protein-swapped dimers together with some preliminary evidence of its impact on their physical and biological properties.

Author Summary

Domain swapping in protein dimers does not always take place by “sticking” a block of one protein onto the surface of the other one. Our analysis reveals that this process often involves a significant intertwining of the two chains, even if they are not particularly long. We show that this entanglement is akin to the topological notion of linking between two closed curves and that it can be quantified by suitable double integrals over the backbones of the proteins. As a practical consequence, if the protein backbones were two ropes, in several cases these would remain linked if their pairs of ends were pulled apart from each other. It appears that Nature has been acting to reduce the linking between long proteins, which are not as linked as their shorter counterparts. Another natural selection result is the presence of some chirality, which on average is negative.

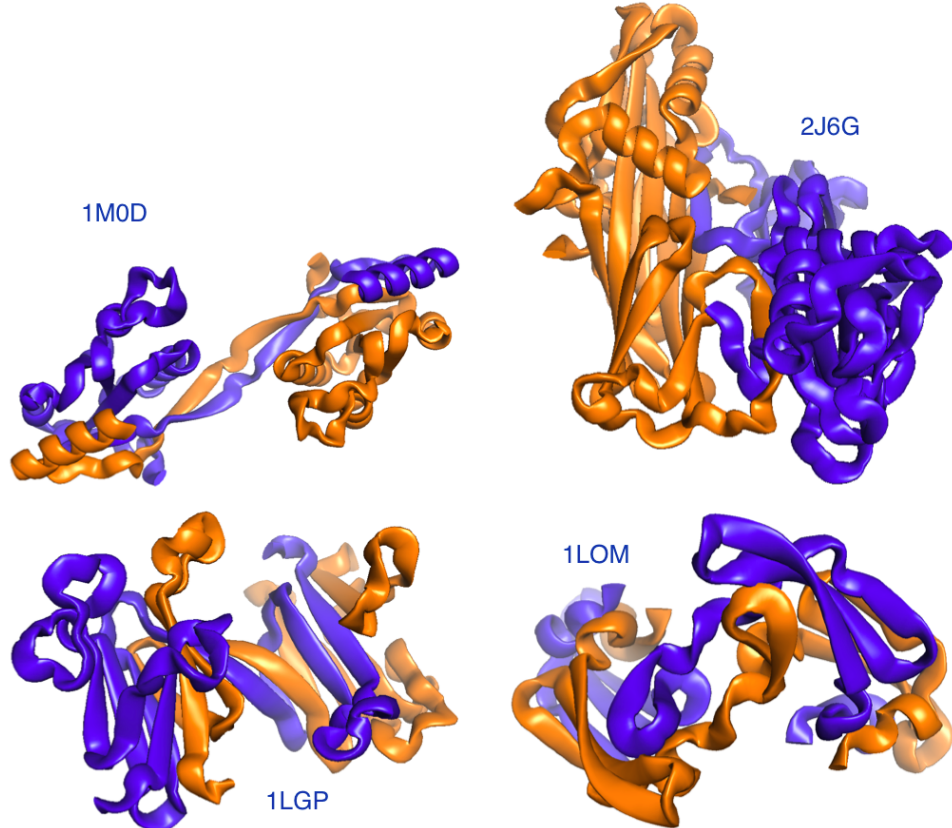


Figure 1. Some domain-swapped dimers with high, negative linking number

1 Introduction

In biological systems, proteins rarely act as isolated monomers and association to dimers or higher oligomers is a commonly observed phenomenon [1–8]. Recent structural and biophysical studies show that protein dimerization or oligomerization is a key factor in the regulation of proteins such as enzymes [9], ion channels [10], receptors and transcription factors [11, 12]. In addition, this mechanism can help to minimize genome size, while preserving the advantages of modular complex formation [3]. Oligomerization, however, can also have deleterious consequences when non-native oligomers, associated with pathogenic states, are generated [13–16]. Specific protein dimerization is integral to biological function, structure and control, and must be under substantial selection pressure to be maintained with such frequency in living organisms.

Protein-protein interactions may occur between identical or non-identical chains (homo or hetero-oligomers) and the association can be permanent or transient [17]. Protein complexes can widely differ based on their affinity. Binding affinities, evaluated for dimers as dissociation constants, can cover up to nine orders of magnitude, highlighting the fact that a strong modulation is necessary to hold up the full protein interaction network [18, 19].

The mechanisms for the evolution of oligomeric interfaces and those for the assembly of oligomers during protein synthesis or refolding remain unclear. Different paradigms have been proposed for the evolution of protein oligomers, among which figures three-dimensional (3D) domain swapping [20–24].

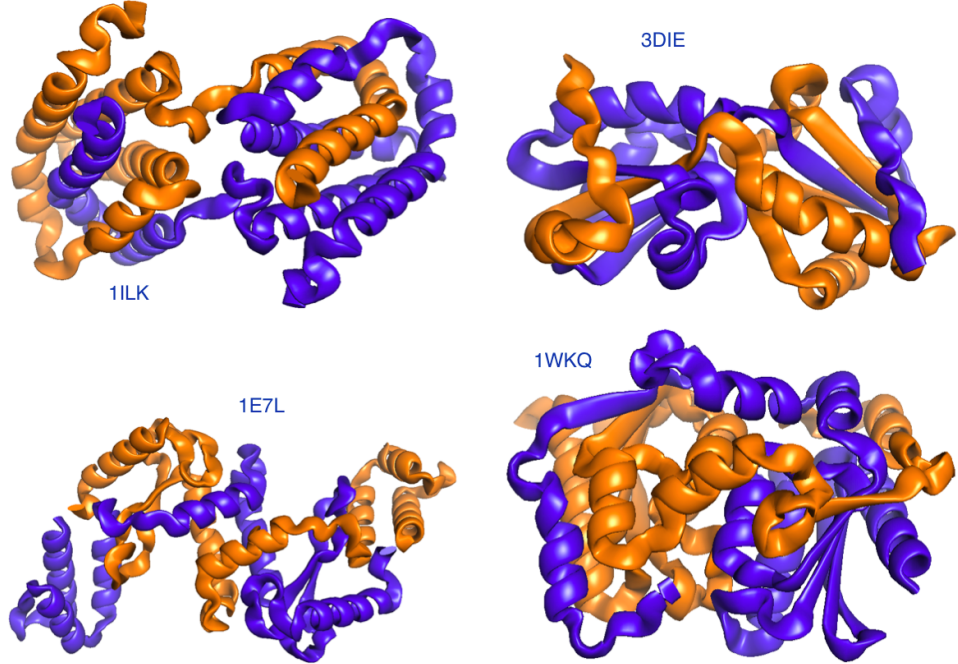


Figure 2. Some domain-swapped dimers with high, positive linking number

Three-dimensional domain swapping is a mechanism through which two or more protein molecules form a dimer or higher oligomer by exchanging an identical structural element (see Figures 1 and 2). Several native (natural/physiological) intra-molecular interactions within the monomeric structures are replaced by inter-molecular interactions of protein structures in swapped oligomeric conformations [25]. Critical in this process is the hinge region, the only polypeptide segment that needs to adopt different conformations in the monomer and in the domain-swapped oligomer. Domain swapping is typically the response of the protein to relieve conformational stress that is present in this hinge region of the monomer. Structures in swapped conformations were reported to perform a variety of functions, and proteins involved in deposition diseases (like neurodegenerative diseases, amyloidosis and Alzheimer's disease) have been reported in 3D domain-swapped conformations [26–29].

Domain-swapped proteins may assume rather complicated spatial structures, since the swapping arms in their rotation can wind up forming tightly compenetrated structures. Examples are shown in Figure 1 and Figure 2. For instance, the *Staphylococcus aureus* thioredoxin (Trx) fold mutant (pdb code 3DIE) represented in Figure 2 clearly illustrates the deep clinging between the two proteins.

The apparent inter-winding between proteins assembled in complexes is certainly a distinguishing characteristic of these systems. An interesting issue to explore is the possibility of introducing topology-based descriptors that can capture the entanglement in a robust and measurable way, and that can be related to either some physico/chemical properties or biological functionalities.

For instance, for single chain globular proteins it has been observed that the backbones may entangle themselves into a physical knot [30–35] that does not disentangle even in the denatured unfolded state [36]. Knotted proteins are interesting because they are rare, and their folding mechanisms and function are not well understood, although it has been proposed that they might increase thermal and kinetic stability [37–39].

Although knots are mathematically defined only for closed loops [40], in the last

decade there have been several attempts to introduce sufficiently robust and topologically inspired measures of knots in open chains [41]. For a single protein, for instance, one can close its backbone by connecting the N and C termini to a point (chosen randomly) on the surface of a sphere that contains the chain. This sphere can be either very large compared to the chain size (closure at infinity) or it can be replaced by the convex hull of the chain. In all cases the artificial closure can introduce additional entanglement and there have been suggested several ways to either mitigate or control this problem [42–44]

For two proteins forming a dimer, if one is interested in measuring the degree of mutual entanglement, the notion of a knotted open chain must be generalised to that of a link between two open chains. In analogy with the procedure used for knots, one can think of closing artificially the two backbones. This can be done by joining the ends of each protein at infinity and computing a link invariant, such as the linking number G , an integer index that detects the degree of homological linking between two closed curves [40]. Note that the two curves are not linked if $G = 0$ while $G = 1$ denotes the simplest link between two loops (Hopf link). Moreover the linking number may be positive or negative depending on the orientation of the two curves. In our implementation we choose to follow the standard N-C orientation along the backbones of the proteins. As in knots, the random closure at infinity may introduce additional entanglement between the two chain and an estimate of G is necessarily a probabilistic one that requires a sufficiently large number of closure paths [43].

Here, in addition to the measure of mutual entanglement based on the estimate of G , we consider an indicator, G' , based simply on the calculation of the Gauss linking integral restricted to the open backbones of the two proteins. Gauss integrals evaluated over the protein backbone were already used successfully as descriptors for classifying single-domain protein chains [45]. Although G' does not derive from a topological notion of linking (no artificial closure is required), we show that it strongly correlates with its topological counterpart G . We use both estimators to analyze a non-redundant set of 3D domain swapped dimers. It turns out that several dimers present a high degree of mutual entanglement.

The short CPU time required to estimate G' allows a quick systematic mining of linked dimers from protein databanks. With a computationally much heavier test, for some dimers we check whether this measure of linking is robust or is just an artifact of the specific crystallographic structure found in the database. This is done by performing simplified molecular dynamics simulations, starting from several native structures with non-trivial values of G' . The time evolution of $G'(t)$ during the process of dissociation of the dimer reveals additional information on the amount of mutual linking.

2 Results

2.1 Databank

Within the protein databank we have found $n_D = 110$ non-redundant domain-swapped proteins and for each of them we have computed the average linking number G and the linking number G' for open chains (see Methods for details, and below). The results are reported in Table 1, ranked for increasing G' . The table also indicates whether the dimer is human (33 cases, tagged with an “h”) or not, and reports the number N of C_α atoms of each protein forming the dimer.

Table 1. Analyzed swapped dimers, ranked from lowest to highest linking G' .

| dimer | G' | G | N | dimer | G' | G | N | dimer | G' | G | N | | |
|-------|-------|-------|-----|-------|-------|-------|-------|-------|------|------|-------|------|-----|
| 1M0D | -2 | -1.65 | 129 | 1K51 | -0.35 | -0.47 | 72 | 1BJ3 | 0.02 | 0 | 129 | | |
| 2J6G | -1.79 | -2.08 | 260 | 2A62 | -0.35 | -0.13 | 319 | 2QYP | 0.02 | 0 | 78 | | |
| 2XDP | -1.75 | -2.23 | 123 | h | 1N9J | -0.35 | -0.32 | 98 | h | 1X2W | 0.03 | 0.01 | 129 |
| 2Z0W | -1.67 | -1.79 | 72 | h | 1K4Z | -0.33 | -0.42 | 157 | 1QB3 | 0.05 | 0 | 113 | |
| 1I1D | -1.42 | -1.26 | 156 | 1TIJ | -0.33 | -0.22 | 114 | h | 1AOJ | 0.09 | 0.29 | 60 | |
| 2P1J | -1.34 | -1.42 | 164 | 1ZVN | -0.32 | -0.13 | 99 | 1S8O | 0.1 | 0.23 | 545 | | |
| 1LGP | -1.32 | -1.28 | 113 | h | 2A4E | -0.28 | -0.25 | 208 | 1CDC | 0.13 | 0.23 | 96 | |
| 1NPB | -1.3 | -1.08 | 140 | 1DXX | -0.27 | -0.17 | 238 | h | 1WY9 | 0.16 | -0.03 | 111 | |
| 1LOM | -1.22 | -1.45 | 101 | 1K04 | -0.27 | -0.63 | 142 | h | 3NG2 | 0.17 | 0.25 | 66 | |
| 2BZY | -1.19 | -1.43 | 62 | h | 3FJ5 | -0.2 | -0.23 | 58 | 2HZL | 0.19 | 0.59 | 338 | |
| 1KLL | -1.16 | -0.78 | 125 | 1CTS | -0.17 | -0.5 | 437 | 2FPN | 0.2 | 2.72 | 198 | | |
| 1HW7 | -1.13 | -1.44 | 229 | 1FOL | -0.17 | -0.35 | 416 | 2CN4 | 0.26 | 0.6 | 173 | | |
| 1BYL | -1.06 | -1.12 | 122 | 2BI4 | -0.15 | -0.02 | 382 | 2SPC | 0.29 | 0.6 | 107 | | |
| 1MI7 | -1.05 | -0.97 | 103 | 2ONT | -0.15 | -0.09 | 73 | h | 1R5C | 0.31 | 0.5 | 124 | |
| 1BUO | -1.03 | -0.99 | 121 | h | 2CI8 | -0.14 | -0.61 | 106 | h | 2CO3 | 0.34 | 0.53 | 142 |
| 1O4W | -0.95 | -1.34 | 123 | 1DWW | -0.12 | -0.29 | 420 | 2OQR | 0.34 | 0.3 | 227 | | |
| 1MU4 | -0.94 | -1.09 | 86 | 1QQ2 | -0.12 | -0.4 | 173 | 1H8X | 0.35 | 0.44 | 125 | | |
| 1W5F | -0.92 | -0.48 | 315 | 1XMM | -0.1 | -0.32 | 288 | h | 3HXS | 0.36 | -0.14 | 120 | |
| 1FRO | -0.88 | -1.08 | 176 | h | 1Q8M | -0.09 | 0.31 | 121 | h | 1GP9 | 0.41 | 0.54 | 170 |
| 2VAJ | -0.88 | -0.52 | 93 | h | 1GT1 | -0.08 | -0.1 | 158 | 2FQM | 0.49 | 0.49 | 65 | |
| 1HT9 | -0.82 | -0.87 | 76 | 1NNQ | -0.07 | 0.26 | 170 | 2DSC | 0.49 | 0.51 | 195 | | |
| 3FSV | -0.79 | -0.38 | 119 | 3D94 | -0.07 | -0.04 | 289 | h | 1SK4 | 0.56 | 0.77 | 162 | |
| 1ZK9 | -0.78 | -0.69 | 110 | 2IV0 | -0.04 | -0.04 | 412 | 2DI3 | 0.62 | 0.49 | 231 | | |
| 3LOW | -0.73 | -0.63 | 100 | h | 2W1T | -0.04 | -0.07 | 175 | 2NZ7 | 0.63 | 0.55 | 93 | |
| 1T92 | -0.66 | -0.61 | 108 | 1L5X | -0.03 | -0.04 | 270 | 2HN1 | 0.66 | 1 | 246 | | |
| 2ES0 | -0.65 | -0.54 | 131 | h | 2E6U | -0.03 | -0.02 | 142 | 1OSY | 0.71 | 1 | 114 | |
| 2RCZ | -0.53 | -0.55 | 79 | h | 2O7M | -0.03 | -0.04 | 153 | 2A9U | 0.76 | 0.86 | 133 | |
| 1KAE | -0.51 | -0.46 | 427 | 4AEO | -0.03 | 0 | 353 | 1A2W | 0.78 | 0.83 | 124 | | |
| 1NIR | -0.51 | -0.5 | 538 | 3PSN | -0.02 | -0.03 | 183 | 1QX7 | 0.81 | 1.08 | 136 | | |
| 1PUC | -0.49 | -0.47 | 101 | 1HE7 | -0.02 | -0.06 | 114 | h | 1QX5 | 0.83 | 1.09 | 145 | |
| 1HUL | -0.49 | -0.66 | 108 | h | 1U4N | -0.01 | 0.3 | 308 | 1MV8 | 0.86 | 1 | 436 | |
| 1I4M | -0.48 | -0.41 | 108 | h | 1UKM | -0.01 | -0.01 | 131 | 1QWI | 0.93 | 1.12 | 140 | |
| 2NU5 | -0.43 | -0.63 | 123 | 1YGT | -0.01 | -0.12 | 104 | 1WKQ | 1.13 | 1.06 | 158 | | |
| 3LYQ | -0.42 | -0.74 | 184 | 1XUZ | 0 | 0.04 | 348 | 1E7L | 1.26 | 1.37 | 166 | | |
| 2GUD | -0.41 | -0.63 | 122 | 2PA7 | 0 | -0.04 | 135 | 3DIE | 1.5 | 1.41 | 106 | | |
| 1R7H | -0.39 | -0.57 | 74 | 1VJ5 | 0 | 0 | 547 | h | 1ILK | 1.68 | 1.63 | 151 | |
| 1ZZK | -0.38 | -0.14 | 96 | 2JFL | 0 | 0 | 286 | h | | | | | |

The mean linking number (G) and the number of amino acids in each protein of the dimer (N) are also reported. Human proteins are tagged with a “h”.

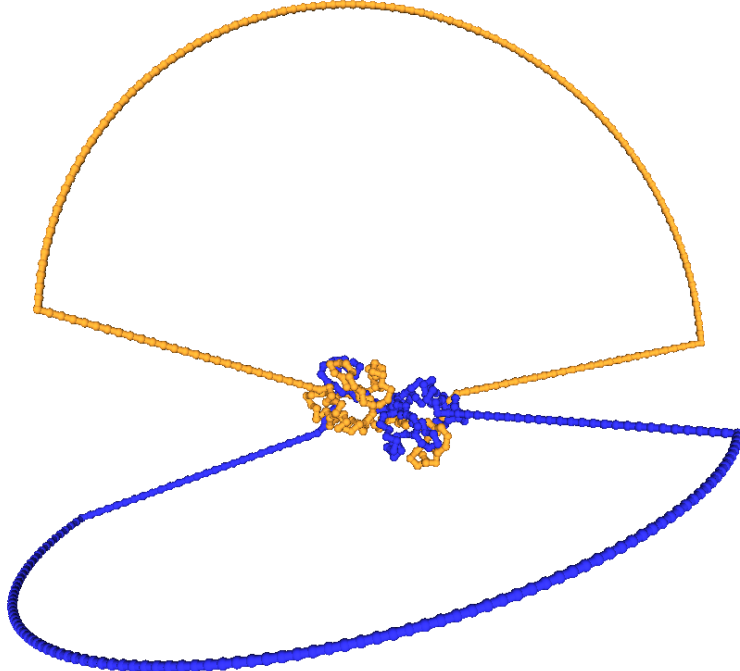


Figure 3. Example of closure in two loops

One of the closures of the 3DIE protein. The other closures of this dimer correspond to different orientations of the semi-circles, hinged to the straight, fixed segments.

2.2 Protein mutual entanglement estimators: G e G'

As a first indicator of the mutual entanglement of two proteins belonging to a given dimer, we consider the Gauss integral G computed over the pair of loops obtained by closing randomly each protein C_α backbones on a sphere (see Figure 3 and Methods for details). For a given closure, G is an integer [40] but, once averaged over several random closures, its mean value G is eventually a fractional number.

Alternatively, we can restrict the calculation of the Gauss integral to the open backbones. This measure, G' , is certainly not a topological invariant but nevertheless it captures the interwinding between the two strands and does not require averages over many random closures. By computing these two quantities on the whole set of swapped domains in our dataset, we can notice that there is a strong correlation between G and G' (see Figure 4). This result validates, at least for the domain-swapped proteins, the use of G' as a faithful measure of the mutual entanglement. The reason to prefer G' is twofold: First, the estimate of G' does not require a computationally expensive averaging over different closure modes. Second, there are cases in which the closure procedure does not work properly, giving rise to an unreasonable value of G (compared to G' , see the point with $G > 2$ and $G' \approx 0$ in Figure 4).

2.3 Analysis of the linking number G'

The histogram reproducing the number of swapped dimers with a given G' is plotted in Figure 5(a): The distribution of G' is fairly well fitted by a Gaussian with mean ≈ -0.1 and standard deviation ≈ 0.63 . The plot has a clear maximum for $G' \approx 0$ suggesting that most of the 3D domain-swapped dimers are not linked. On the other hand, there is a consistent percentage of structures that exhibit a non trivial value of $|G'|$. In

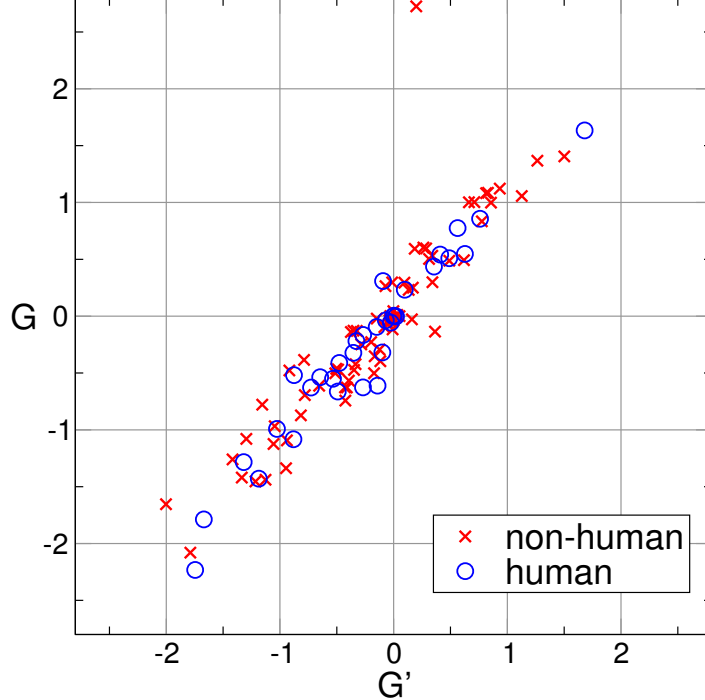


Figure 4. Correlation between the two measures of linking.

Except for an outlier point, data show a good linear correlation between G and G' .

particular, in Table 1 there are 15 structures with $G' < -1$ and 4 dimers have $G' > 1$. Hence, more than 15% of the dimers in our databank have $|G'|$ higher than 1.

The figures also tell us that the statistics of mutual entanglement displays an asymmetry towards more negative values of G' . Indeed, in Table 1 one could notice that about two thirds of the dimers have $G' < 0$. For obtaining a better evaluation of the spread and average value of G' , we analyzed the empirical cumulative distribution function $F(G')$, namely the fraction of configurations that have a value at most equal to G' , see solid lines in Figure 5(b). These have been fitted by an error-function with non-zero average. The fit yields average $G'_0 = -0.163$ and standard deviation $\Delta G' = 0.853$ (the corresponding fit is shown as a dashed line in Figure 5(b)). If the fit is restricted to non-human dimers, we get $G'_0 = -0.130$ and $\Delta G' = 0.830$, while for the human dimers we get $G'_0 = -0.237$ and $\Delta G' = 0.839$. Again, mean values are lower than zero both for the case of human proteins and non-human ones. A fraction of data $\approx 64\%$ (non-humans) and $\approx 70\%$ (humans) have $G' < 0$.

The asymmetry in the distribution in favor of structures with negative G' is slightly more marked for human swapped dimers. This could be explained by the fact that, for human proteins, the interface between the secondary structures of the two monomers is mainly formed by swapped β -structures: the preferential right-handed twist of the β -sheets together with the higher frequency of anti-parallel pairings may imply a negative value for G' .

In order to verify whether our definition of linking number is affected by some bias that can be introduced by the different lengths of proteins, in Figure 6 we plot G' as a function of the number of amino acids in the proteins forming the dimers. As a matter of fact we see that the mean value of $|G'| \approx 1/2$ is not varying significantly in the range under investigation, which includes protein lengths ranging from about 50 to 1000 amino acids. Only fluctuations are larger at small length due to the presence of more data. Therefore we conclude that, in our dataset, the linking number is a robust

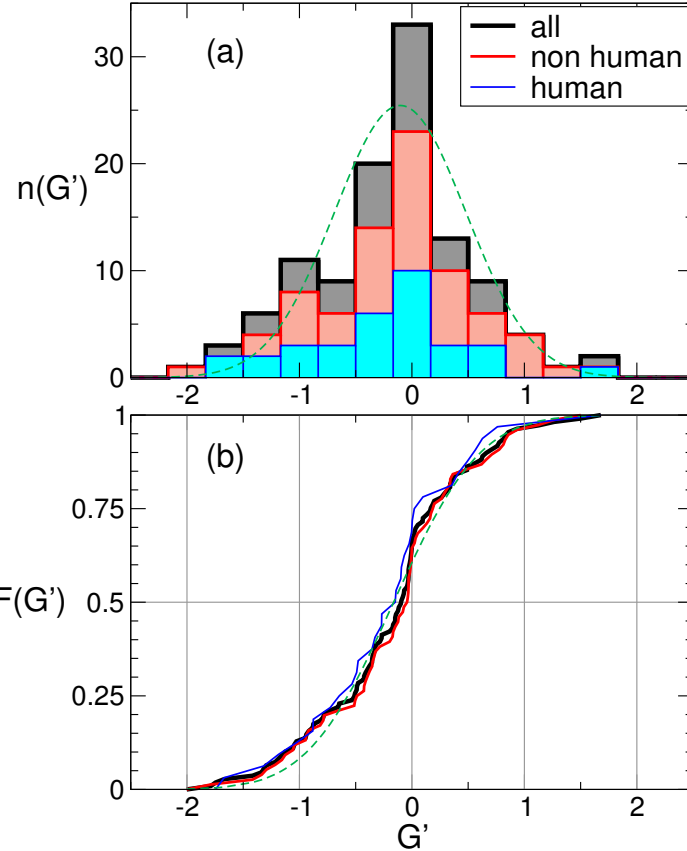


Figure 5. Distribution of the linking.

(a) Histogram of the values of G' for all swapped dimers in the database, and contributions from the groups of human and non-human dimers. The global histogram is fitted by a Gaussian distribution (dashed line) with mean $m \approx -0.1$ and standard deviation $\sigma \approx 0.63$. (b) Cumulative distributions of G' for the same ensembles (solid lines) and an error function fit of the the global set of data (dashed line).

parameter intrinsic to the dimers and it is not affected by entropic effects induced by the length of the protein.

2.4 Dynamical linking number

The values of G' are easy to compute from configurations and thus represent a basic indicator of the linking of a structure. Through visual inspection of configurations, as those shown in Figure 1 and Figure 2, one verifies indeed that dimers with large $|G'|$ are quite intertwined. However, from the same figures, it appears that, in addition to a global twisting of one protein around the other, G' may be affected by some local details of the chains, such as their 3D shape near their ends. These local details should be irrelevant if one thermally excites the dimer, which should unfold with a time scale that corresponds to the Rouse dynamics needed to untwist one whole chain from the other [46].

Motivated by these observations, to complement G' we tackle the problem of the linking from a dynamical perspective. For some test dimers we monitor the evolution of the value of $G'(t)$ with time, in a Langevin simulation where only excluded volume effects play a role (besides of course the chain connectivities). This is equivalent to the

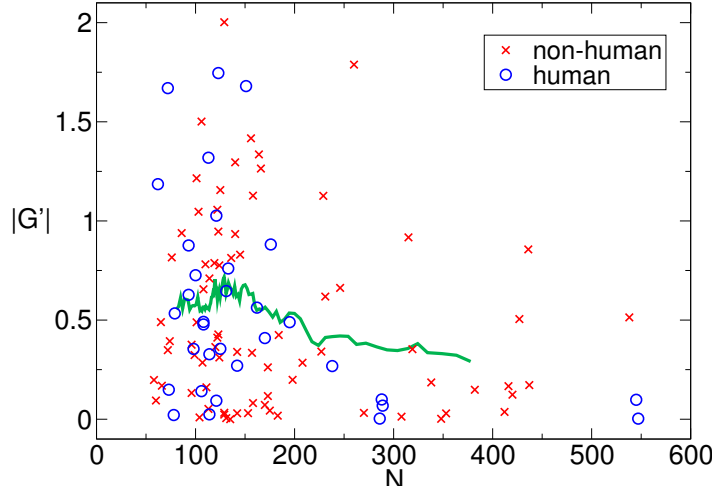


Figure 6. Modulus of the linking number vs. protein length.

Absolute linking number G' as a function of the number of amino acids in one protein of a dimer. The line represents a running average over 21 points.

Table 2. Relaxation time τ and linking numbers, for some swapped dimers.

| dimer | N | τ | G^* | G' | G |
|-------|-----|-----------|-------|-------|-------|
| 1MOD | 129 | 1000(70) | -1.25 | -2.00 | -1.65 |
| 1LGP | 113 | 1140(80) | -1.70 | -1.33 | -1.28 |
| 1LOM | 101 | 660(80) | -0.77 | -1.23 | -1.46 |
| 1WKQ | 155 | 2500(120) | 0.72 | 1.13 | 1.07 |
| 3DIE | 107 | 1090(90) | 1.68 | 1.50 | 1.41 |

unfolding at a sufficiently high temperature.

The average curve of $G'(t)$ over many trajectories starts from the static value of the crystallographic structure ($G'(0) = G'$) and decays to zero for long time. It turns out that an exponential form $G^*e^{-t/\tau}$ represents well the long time decay of $G'(t)$. However, the extrapolated value of the fit at time $t = 0$, namely G^* , does not necessarily match the static value G' . In the studied cases, shown in Figure 7 and listed in Table 2, we find both instances of $|G^*| > |G'|$ (3DIE and 1LGP), and $|G^*| < |G'|$ (1WKQ, 1LOM, 1M0D). This shows that G^* , a more time consuming option than G' , may however be considered for complementing the quick, static evaluation of the linking. Of course, any dynamical procedure provides a result that depend on the kind of dynamics used to disentangle the structure. For example, we may expect different G^* from room temperature all atom molecular dynamics [47] or Monte-Carlo methods based on local moves [48], where effective interactions among amino-acids are taken into account. Hence, the analysis of dimers' linking through the value of G' may, and should, be complemented by alternative dynamical methods, in order to get a detailed picture of the entanglement conditions.

The second parameter of the fit, the timescale τ (in simulation units), should increase with the chain length. This is expected for Rouse dynamics of polymers in general [46]: to shift the polymer center of mass of one radius of gyration one needs to wait a time $\sim N^{2\nu+1}$ with Flory exponent $\nu \approx 3/5$. It is not possible for us to asses if this scaling is respected, given the few cases analyzed. However, these cases correctly display an almost monotonically increasing trend of τ with N (compatibly with error bars, see Table 2). Note that strong logarithmic corrections to the scaling $\tau \sim N^{2\nu+1}$ are also expected in unwinding processes [49, 50].

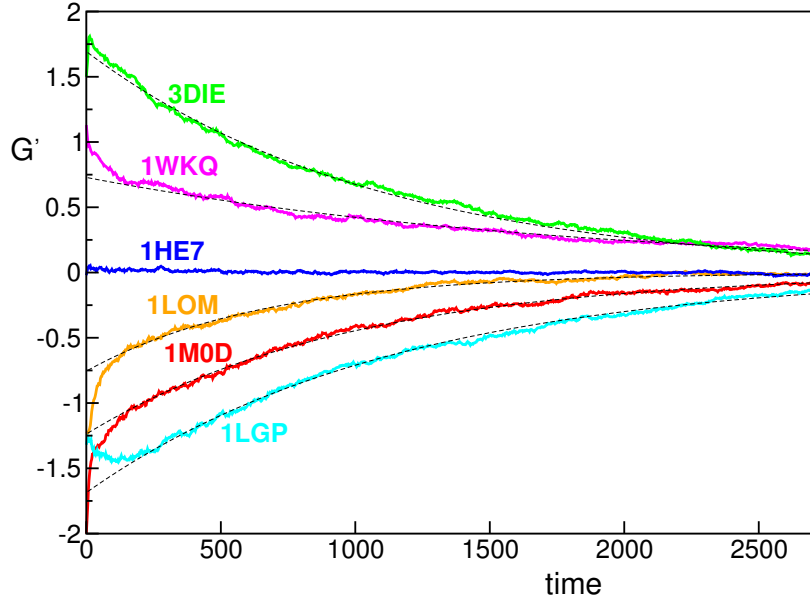


Figure 7. Decay of the linking number with time, during unfolding.

Time dependence of G' during the unfolding dynamics of a set of swapped dimers. The dashed curves correspond to the best fit of the data with the function $G^* \exp(-t/\tau)$. Note that, to better catch the exponential decay, the first 100 time steps have been neglected in the fit.

Discussion

Mathematically, two curves are linked or not, in a rigorous sense, only if they are loops. Hence, it is not trivial to estimate the level of linking between two open chains. Yet, the mutual entanglement is a well-visible feature in the crystallographic structures of several domain-swapped dimers. Being interested in quantifying such entanglement, with Gauss double integrals over the backbones of the two proteins in the dimers we provide a simple and efficient way for computing the amount of linking, as expressed by the linking number G' . Indeed, according to our comparisons, a procedure for looping each protein (with an artificial continuation escaping from the core of the dimer) produces on average a linking number G that is strongly correlated with G' . This suggests that such procedure can be avoided in practice, one may just rely on the information from the open chains, encoded in G' .

We report that about 15% of the domain-swapped dimers have a significant linking $|G'| > 1$. This is quite intriguing, especially if compared with corresponding figures for knotting of single proteins, where about 1% of the PDB entries has been found to host a knot [34].

The asymmetry in the typical values of G' , with many more cases with $G' < 1$ than with $G' > 1$, is another interesting feature emerging from our analysis. This asymmetry could be explained by the conjecture that the linking number, despite being a global topological feature, can be deduced from the local twistings of closely interacting swapped structural elements. In several cases the latter are β -strands within the same sheet (see for example 1MOD, 1LGP in Figure 1 and 3DIE, 1WKQ in Figure 2), so that the more frequent case of a right-handed anti-parallel β -sheet [51] would indeed imply a negative linking number. With a preliminary overview, we note that anti-parallel swapped β -sheets are indeed occurring more frequently in the human dimers of our database than in the non-human ones, and human dimers have indeed on average a

more negative G' . The dependence of the linking number of domain-swapped protein dimers on the local twist of swapped interacting elements is a feature clearly worth further investigation. If confirmed, the tuning of local interactions could then be an evolutionary mechanism used by natural selection to control the emergence of topological entanglement in domain-swapped dimers.

The longer the proteins in the dimers, the slightly lower is their linking. This is a surprising feature because one might anticipate that longer chains should be more easily entangled than shorter ones. Thus, it seems that the natural selection has acted against a form of random linking in long domain-swapped protein dimers.

Via numerical simulations of the dissociation of some dimers, we observe that the presence of a non-trivial mutual entanglement is a robust characteristic, which vanishes exponentially with time during the dimer unbinding. The exponential fit furnishes a characteristic disentanglement time τ whose values does not depend on G' and is weakly correlated with the length of the proteins. The amplitude of the exponential decay of the linking furnishes a further estimate (G^*) of the linking in the dimer, which complements the G' of the crystallographic structure (they are not exactly equal to each other) in assessing the amount of linking in the dimer.

Our new approach of classifying domain-swapped protein dimers according to their mutual entanglement will likely add novel insight on the crucial role played by the generic topological properties of linear polymer chains in the protein context. As already demonstrated in the case of knotted protein folds [35], the presence of a global topological constraint, such as the linking between two protein chains, may strongly impact the conformational properties, the thermodynamic and kinetic stability, the functional and evolutionary role of domain-swapped structures.

Finally, it is interesting to speculate on the possible outcome of a single-molecule experiment performed by pulling apart the two protein backbones of a domain-swapped dimer with significant linking (high $|G'|$). A similar experiment was carried on very recently for single-domain protein knots, showing that the knotting topology of the unfolded state can be controlled by varying the pulling direction [57]. In the linked dimer case, similarly, we expect the choice of the pulling directions to be crucial in allowing or not dimer unlinking and dissociation into monomers.

Materials and Methods

Data bank of 3D domain-swapped dimers

In order to derive a statistically significant ensemble of non-redundant domain-swapped dimers, we merge two existing databanks of domain-swapped proteins, namely *3Dswap* [52–54] and *ProSwap* [55, 56]. These databanks provide curated information and various sequence and structural features about the proteins involved in the domain swapping phenomenon. PDB entries involved in 3D Domain swapping are identified from integrated literature search and searches in PDB using advanced mining options. We first consider only the dimers and, to avoid the presence of related structures, we consider the UniprotKB code. For each code, we select only one protein, the one obtained experimentally with the highest experimental accuracy. We then filter the remaining structures to avoid the presence of holes in the main backbone chain. Specifically, we discarded those proteins in which the distance between two C_{α} , listed consecutively in the pdb file, is bigger than 10 Å. As a matter of fact, such holes could affect dramatically the reliability of the linking numbers and there is not an obvious strategy to join them artificially. At the end we obtained a databank of $n_D = 110$ proteins, whose PDB code is reported in Table 1. Out of these, 33 were human.

Gauss integrals

Our procedure for estimating the amount of linking between two proteins uses Gauss integrals. As representative of the backbones of proteins, we consider the chains connecting the coordinates \vec{r} of the C_α atoms of amino acids, which are N in each of the two proteins in the dimer.

A definition of linking number between two closed curves γ_1 and γ_2 in 3 dimensions is given by the Gauss (double) linking integral,

$$\mathcal{G} \equiv \frac{1}{4\pi} \oint_{\gamma_1} \oint_{\gamma_2} \frac{\vec{r}^{(1)} - \vec{r}^{(2)}}{|\vec{r}^{(1)} - \vec{r}^{(2)}|^3} \cdot (d\vec{r}^{(1)} \times d\vec{r}^{(2)}) \quad (1)$$

This formula yields integer numbers $\mathcal{G} = 0, -1, 1, -2, 2$, etc. Such definition is adapted to compute the amount of linking between two proteins. We need first to define a procedure that closes each open chain via the addition of artificial residues. This closure starts by computing the center of mass of the dimer and by considering such center as a repeller for the new growing arms. Let us describe the method for protein 1, as for protein 2 it is exactly the same: from each of the two free ends we continue with a path expanding diametrically from the center of mass, with a length corresponding to $n = 25$ typical $C_\alpha - C_\alpha$ distances $\ell \approx 3.8 \text{ \AA}$. At this stage the polymer is composed by $N + 2n$ residues. Since there is some arbitrariness in the final closure joining the two artificial new end residues, we perform a statistics over 12 different closures, each being a meridian along a sphere where the poles are the artificial end residues. Semicircular closure paths are drawn, each containing a number of artificial residues n' that makes their bond distance as close as possible to ℓ . An example is shown in Figure 3.

Each closed chain becomes a collection of $N_{\text{tot}} = N + 2n + n'$ points $\{\vec{r}_1^{(1)}, \vec{r}_2^{(1)}, \dots, \vec{r}_N^{(1)}, \vec{r}_{N+1}^{(1)}, \dots, \vec{r}_{N_{\text{tot}}}^{(1)}\}$ separated by about a fixed spacing $|\vec{r}_{i+1} - \vec{r}_i| \approx \ell$, so that the integrals are replaced by sums over segments $d\vec{R}_i^{(1)} = \vec{r}_{i+1}^{(1)} - \vec{r}_i^{(1)}$, for which we use the midpoint approximation $\vec{R}_i^{(1)} \equiv (\vec{r}_{i+1}^{(1)} + \vec{r}_i^{(1)})/2$. For a given choice z of the closure for both proteins, out of the $\mathcal{Z} = 12 \times 12 = 144$ possible ones, we have

$$\mathcal{G}_z \equiv \frac{1}{4\pi} \sum_{i=1}^{N_{\text{tot}}} \sum_{j=1}^{N_{\text{tot}}} \frac{\vec{R}_i^{(1)} - \vec{R}_j^{(2)}}{|\vec{R}_i^{(1)} - \vec{R}_j^{(2)}|^3} \cdot (d\vec{R}_i^{(1)} \times d\vec{R}_j^{(2)}) \quad (2)$$

(indices run periodically, hence $N_{\text{tot}} + 1 \rightarrow 1$, and the notation leaves the dependence of \vec{R} 's on z understood), and the final estimate of linking is an average over \mathcal{Z} closures

$$G = \frac{1}{\mathcal{Z}} \sum_{z=1}^{\mathcal{Z}} \mathcal{G}_z. \quad (3)$$

A closure provides an integer linking number \mathcal{G}_z , though the final average G may become not integer if closures with different \mathcal{G}_z are generated. As an alternative, we relax the requirement to have basic integer indicators of linking and we perform the double Gauss discrete integral over the open chains. The indicator

$$G' \equiv \frac{1}{4\pi} \sum_{i=1}^{N-1} \sum_{j=1}^{N-1} \frac{\vec{R}_i^{(1)} - \vec{R}_j^{(2)}}{|\vec{R}_i^{(1)} - \vec{R}_j^{(2)}|^3} \cdot (d\vec{R}_i^{(1)} \times d\vec{R}_j^{(2)}) \quad (4)$$

has no statistical averaging and is a straightforward alternative to G in the estimate of the linking of proteins.

Simulations

In our molecular dynamics simulations, each protein forming the dimer is modeled as a self-avoiding chain of N beads. Each bead has radius σ and is centered in the C_α position of a residue. Adjacent beads of each protein are tethered together into a polymer chain by an harmonic potential with the average C_α - C_α distance along the chain equal to 1.5σ . To take into account the excluded volume interaction between beads we consider the truncated Lennard-Jones potential

$$U_{\text{LJ}} = \sum_{i,j>i}^N 4\epsilon \left[\left(\frac{\sigma}{d_{i,j}} \right)^{12} - \left(\frac{\sigma}{d_{i,j}} \right)^6 + \frac{1}{4} \right] \theta(2^{1/6}\sigma - d_{i,j}) \quad (5)$$

where $d_{i,j} = |\vec{r}_i - \vec{r}_j|$ is the distance of the bead centers i and j , θ is the Heaviside function and ϵ is the characteristic unit of energy of the system which is set equal to the thermal energy $k_B T$.

The system dynamics is described within a Langevin scheme:

$$m\ddot{\vec{r}}_i = -\gamma\dot{\vec{r}}_i - \nabla U_i + \vec{\eta}_i \quad (6)$$

where U_i is the total potential of the i th particle, γ is the friction coefficient and η is the stochastic delta-correlated noise. The variance of each Cartesian component of the noise, σ_η^2 satisfies the usual fluctuation dissipation relationship $\sigma_\eta^2 = 2\gamma k_B T$. As customary, we set $\gamma = m/(2\tau_{LJ})$, with $\tau_{LJ} = \sigma\sqrt{m/\epsilon} = \sigma\sqrt{m/k_B T}$ being the characteristic simulation time. From the Stokes friction coefficient of spherical beads of diameters σ we have $\gamma = 3\pi\eta_{sol}\sigma$, where η is the solution viscosity. By using the nominal water viscosity, $\eta_{sol} = 1cP$ and setting $T = 300\text{K}$ and $\sigma = 2.5\text{nm}$, one has $\tau_{LJ} = 6\pi\eta_{sol}\sigma^3/\epsilon = 74\text{ns}$.

To study the unfolding dynamics of a given dimer we take its folded configuration, as given by the PDB, as the initial condition. For each initial condition we generate 100 different molecular dynamics trajectories by integrating numerically (6) up to $t = 10^4\tau_{LJ}$. During the dynamics we monitor the quantities G and G' . In Figure 7 the curves are obtained by averaging over the 100 trajectories.

References

1. Nussinov R, Jang H, Tsai CJ (2015) Oligomerization and nanocluster organization render specificity. *Biol Reviews* 90:587-598.
2. MacKinnon SS, Wodak SJ (2015) Landscape of intertwined associations in multi-domain homo-oligomeric proteins. *J Mol Biol* 427:350-370.
3. Marianayagam NJ, Sunde M, Matthews JM (2004) The power of two: protein dimerization in biology. *Trends Biochem Sci* 29:618-625.
4. Deremble C, Lavery R (2005) Macromolecular recognition. *Current Opin Struct Biol* 15:171-175.
5. Ellis RJ (2001) Macromolecular crowding: obvious but underappreciated. *Trends Biochem Sci* 26:597-604.
6. Ouzounis CA, Coulson RM, Enright AJ, Kunin V, Pereira-Leal JB (2003) Classification schemes for protein structure and function. *Nature Rev Genet* 4:508-519.
7. Worth CL, Gong S, Blundell TL (2009) Structural and functional constraints in the evolution of protein families. *Nature Rev Mol Cell Biol* 10:709-720.

8. Wodak SJ, Janin J (2002) Structural basis of macromolecular recognition. *Adv Prot Chem* 61:9-73.
9. Bonafe CF, Matsukuma AY, Matsuura MS (1999) ATP-induced tetramerization and cooperativity in hemoglobin of lower vertebrates. *J Biol Chem* 274:1196-1198.
10. Hébert TE, Bouvier M (1998) Structural and functional aspects of G protein-coupled receptor oligomerization. *Biochem Cell Biol* 76:1-11.
11. Pingoud A, Jeltsch A (2001) Structure and function of type II restriction endonucleases. *Nucl Acids Res* 29:3705-3727.
12. Beckett D (2001) Regulated assembly of transcription factors and control of transcription initiation. *J Mol Biol* 314:335-352.
13. Viola KL, Klein WL (2015) Amyloid β oligomers in Alzheimer's disease pathogenesis, treatment, and diagnosis. *Acta Neuropathol* 129:183-206.
14. Knowles TP, Vendruscolo M, and Dobson CM (2014) The amyloid state and its association with protein misfolding diseases. *Nature Rev Molec Cell Biol* 15:384-396.
15. Fändrich M (2012) Oligomeric intermediates in amyloid formation: structure determination and mechanisms of toxicity. *J Mol Biol* 421, 427-440.
16. Kayed R, Head E, Thompson JL, McIntire TM, Milton SC, Cotman CW, and Glabe CG (2003) Common structure of soluble amyloid oligomers implies common mechanism of pathogenesis. *Science* 300:486-489.
17. Ali, A, and Bagchi, A (2015) An Overview of Protein-Protein Interaction. *Curr Chem Biol* 9:53-65.
18. Kastritis PL, Moal IH, Hwang H, Weng Z, Bates PA, Bonvin AM, Janin J (2011) A structure-based benchmark for protein–protein binding affinity. *Prot Sci* 20:482-491.
19. Kastritis PL, Bonvin AM (2013) On the binding affinity of macromolecular interactions: daring to ask why proteins interact. *J Royal Soc Interface* 10:20120835.
20. Jaskolski M (2013) 3D Domain swapping. In *Encyclopedia of Biophysics* (pp. 1-7), Springer Berlin Heidelberg.
21. Bennett MJ, Choe S, Eisenberg D (1994) Domain swapping: entangling alliances between proteins. *Proc Natl Acad Sci USA* 91:3127-3131
22. Green SM, Gittis AG, Meeker AK, Lattman EE (1995) One-step evolution of a dimer from a monomeric protein. *Nature Struct Mol Biol* 2:746-751.
23. Bennett MJ, Schlunegger MP, Eisenberg D (1995) 3D domain swapping: a mechanism for oligomer assembly. *Protein Sci* 4:2455-2468.
24. Liu Y, Eisenberg D (2002) 3D domain swapping: as domains continue to swap. *Protein Sci* 11:1285-1299.
25. Yang S, Levine H and Onuchic JN (2005) Protein oligomerization through domain swapping: role of inter-molecular interactions and protein concentration. *J Mol Biol* 352:202-211.

26. Alva V, Ammelburg M, Söding J, Lupas AN (2007) On the origin of the histone fold. *BMC Struct Biol* 7:17.
27. Jaskólski M (2001) 3D domain swapping, protein oligomerization, and amyloid formation. *Acta Biochim Polonica-English Edition-* 48:807-828.
28. Liu Y, Gotte G, Libonati M, Eisenberg D (2001) A domain-swapped RNase A dimer with implications for amyloid formation. *Nat Struct Mol Biol* 8:211-214.
29. Rousseau, F, Schymkowitz, J, and Itzhaki, LS (2012) Implications of 3D domain swapping for protein folding, misfolding and function. In *Protein Dimerization and Oligomerization in Biology* (pp. 137-152) Springer New York.
30. Mansfield ML (1997) Fit to be tied. *Nat Struct Mol Biol* 4:166-167.
31. Taylor WR (2000) A deeply knotted protein structure and how it might fold. *Nature* 406:916-919.
32. Virnau P, Mirny L, Kardar M (2006) Intricate knots in proteins: Functin and Evolution. *PLoS Comput Biol* 2:1074-1079.
33. Lua RC, Grosberg AY (2006) Statistics of knots, geometry of conformations, and evolution of proteins. *PLoS Comput Biol* 2:e45
34. Jamroz M, Niemyska W, Rawdon EJ, Stasiak A, Millett KC, Sulkowski P, Sulkowska JI (2014) KnotProt: a database of proteins with knots and slipknots. *Nucl Acids Res* 43(DI):D306-D314
35. Lim NCH, Jackson SE (2015) Molecular knots in biology and chemistry. *J Phys Cond Mat* 27:354101
36. Mallam AL, Rogers JM, Jackson SE (2010) Experimental detection of knotted conformations in denatured proteins. *Proc Natl Acad Sci USA* 107:8189–8194.
37. Sułkowskaa JI, Sułkowskic P, Szymczake P, Cieplak M (2008) Stabilizing effect of knots on proteins. *Proc Natl Acad Sci USA* 105:19714–19719.
38. Mallam AL, Morris ER, Jackson SE (2008) Exploring knotting mechanisms in protein folding. *Proc Natl Acad Sci USA* 105:18740–18745.
39. Soler MA, Faisca FN (2013) Effects of Knots on Protein Folding Properties. *PLoS Comput Biol* 8:e74755.
40. Rolfsen D (1976) Knots and Links. *Mathematics Lecture Series* 7, Publish or Perish, Inc., Houston, Texas.
41. Orlandini E, Whittington SG (2007) Statistical topology of closed curves: Some applications in polymer physics. *Rev Mod Phys* 79:611-642.
42. Marcone B, Orlandini E, Stella AL, Zonta F (2005) What is the length of a knot in a polymer? *J Phys A: Math Gen* 38:L15-L21.
43. Millett K, Dobay A, Stasiak A (2005) Linear random knots and their scaling behavior. *Macromolecules* 38:601-606.
44. Tubiana L, Orlandini E, Micheletti C (2011) Profiling the arc entanglement of compact ring polymers: a comparison of different arc-closure schemes with applications to knot localization. *Prog Theor Phys* 191:192-204.

45. Rogen P, Fain B (2004) Automatic classification of protein structure by using Gauss integrals. *Proc Natl Acad Sci USA* 100:119-124.
46. Doi M, Edwards SF (1986) The Theory of Polymer Dynamics, Oxford University Press, USA.
47. Cossio P, Granata D, Laio A, Seno F, Trovato A (2012) A simple and efficient statistical potential for scoring ensembles of protein structures. *Sci Rep* 2:351.
48. Zamuner, S, Rodriguez A, Seno F, Trovato A (2015) An efficient algorithm to perform local concerted movements of a chain molecule. *PLoS one* 10:e0118342.
49. Walter JC, Baiesi M, Barkema GT, Carlon E (2013) Unwinding Relaxation Dynamics of Polymers. *Phys Rev Lett* 110:068301
50. Water JC, Baiesi M, Carlon E, Schiessel H (2014) Unwinding Dynamics of a Helically Wrapped Polymer. *Macromolecules* 47:4840-4846
51. Cheng P-N, Pham JD, Nowick JS (2013) The Supramolecular Chemistry of β -Sheets. *J Am Chem Soc* 135:5477-5492.
52. Shameer K, Pugalenth G, Kumar Kandaswamy K, Sowdhamini R (2011) 3dswap-pred: prediction of 3D domain swapping from protein sequence using random forest approach. *Prot Pept Lett* 18:1010-1020.
53. Shameer K, Shingate PN, Manjunath SCP, Karthika M, Pugalenth G, Sowdhamini R (2011) 3DSwap: curated knowledgebase of proteins involved in 3D domain swapping. *Database J Biol Datab Curat* bar042. PMID: 21959866
54. <http://caps.ncbs.res.in/3DSwap/>
55. Turinsky AL, Razick S, Turner B, Donaldson IM, Wodak SJ (2011) Interaction databases on the same page. *Nature Biotech* 29:391-393.
56. <http://wodaklab.org/proswap/>
57. Ziegler F, Limb NCH, Mandal SS, Pelz B, Ng W-P, Schlierf M, Jackson SE, Rief M (2016). Knotting and unknotting of a protein in single molecule experiments *Proc Natl Acad Sci USA* in press, doi:10.1073/pnas.1600614113.